Scattering of 217-Mev Negative Pions by Hydrogen†*

MAURICE GLICKSMAN
Institute for Nuclear Studies, University of Chicago, Chicago, Illinois
(Received January 18, 1954)

The differential cross sections for scattering of 217-Mev negative pi mesons by liquid hydrogen have been observed at six angles. An analysis of the angular distribution of the ordinary scattering is consistent with a small d-wave contribution; the charge exchange scattering angular distribution agrees with the assumption of only s and p waves. The integrated total cross sections are $18.2\pm2.3\times10^{-27}$ cm^2 for the ordinary scattering and $35.8\pm3.4\times10^{-27}$ cm^2 for the charge exchange scattering. Transmission measurements of the total cross section gave values of $57.2\pm2.9\times10^{-27}$ cm^2 at 209 Mev and $52.1\pm2.3\times10^{-27}$ cm^2 at 220 Mev. An analysis of the angular distributions in terms of phase shifts is discussed.

A STUDY of the pion scattering reactions

$$\pi^+ + p \rightarrow \pi^+ + p, \quad (1)$$

$$\pi^- + p \rightarrow \pi^- + p, \quad (2)$$

$$\pi^- + p \rightarrow \pi^0 + n, \quad (3)$$

is of considerable value in understanding the interaction between pions and nucleons. Angular distributions for these reactions have been reported by a number of authors.[1–9] On the basis of charge independence, the scattering should be describable in terms of phase shifts. At low energies, angular momentum states higher than s or p waves may be assumed unimportant. One set of six phase shifts should then completely describe the scattering at a definite energy.

An extensive study of these reactions has been made at 120 and 135 Mev by AFMN.[5] Their results enable them to eliminate all but two possible sets of phase shifts. Observations of the scattering of negative pions alone at higher energies (up to 210 Mev) have been reported.[8] A phase shift analysis of these data is more difficult.[10] Because of the higher energy, it is quite possible that d states contribute appreciably to the scattering and need to be included in the analysis. It is also not possible to calculate a unique set of phase shifts from the negative scattering data alone. Some positive scattering data at high energies have recently become available[9–12] and an analysis using these data may prove successful in limiting the number of sets of phase shifts which agree with the negative pion scattering observations.

It was felt that it would be worthwhile making detailed measurements of the negative and positive pion scattering at an energy in the 210-Mev region. A detailed differential cross section should give some information on the importance of d waves and good measurements of both positive and negative differential cross sections should remove the ambiguity in the phase-shift analysis. This paper reports observations of the differential cross sections of reactions (2) and (3) for an incident pion energy of 217 Mev. The scattered pions from (2) and the gamma rays resulting from the decay of the π^0 in (3) (plus a small contribution from the reaction $\pi^- + p \rightarrow \gamma + n$) were observed at six angles. Within the limits of error of the experiment, this allows some test of the validity of an analysis in terms of s and p waves alone; an experiment on the positive pion scattering at the same energy is now being carried out here by others.

I. EXPERIMENTAL ARRANGEMENT

The arrangement is essentially the same as that used in previous work.[5] The pions were produced by the bombardment of a beryllium target by the internal 450-Mev proton beam of the Chicago synchrocyclotron. Pions of nominal energy 227 Mev are deflected out of the cyclotron and focussed in a fairly parallel beam by the fringing magnetic field. They traverse a channel through the twelve feet of shielding and are then deflected by a steering magnet into the detecting scintillation counters. A description of the pion beams, target and steering magnet has been published.[13]

Details of the scattering geometry are given in Fig. 1. The pions incident on the liquid hydrogen were detected by two 2-inch diameter scintillation counters (No. 1 and No. 2) with the second counter 5.5 inches from the center of the liquid hydrogen cell. Scattered pions (and a small number of converted gamma rays)

† Research supported by a joint program of the U. S. Office of Naval Research and the U. S. Atomic Energy Commission.
* Submitted to the Department of Physics, the University of Chicago in partial fulfillment of the requirements for the Ph.D. degree.
[1] Anderson, Fermi, Nagle, and Yodh, Phys. Rev. **86**, 793 (1952).
[2] Fowler, Fowler, Shutt, Thorndike, and Whittemore, Phys. Rev. **86**, 1053 (1952).
[3] G. Goldhaber, Phys. Rev. **89**, 1187 (1953).
[4] Bodansky, Sachs, and Steinberger, Phys. Rev. **90**, 996, 997 (1953).
[5] Anderson, Fermi, Martin, and Nagle, Phys. Rev. **91**, 155 (1953), quoted here as AFMN.
[6] J. P. Perry and C. E. Angell, Phys. Rev. **91**, 1289 (1953).
[7] J. Orear, Phys. Rev. **92**, 156 (1953).
[8] Fermi, Glicksman, Martin, and Nagle, Phys. Rev. **92**, 161 (1953).
[9] Fowler, Lea, Shephard, Shutt, Thorndike, and Whittemore, Phys. Rev. **92**, 832 (1953).
[10] E. Fermi (private communication).
[11] Homa, Goldhaber, and Lederman, Phys. Rev. **93**, 554 (1954).
[12] R. A. Grandey and A. F. Clark (private communication).
[13] R. L. Martin, Phys. Rev. **87**, 1052 (1952).

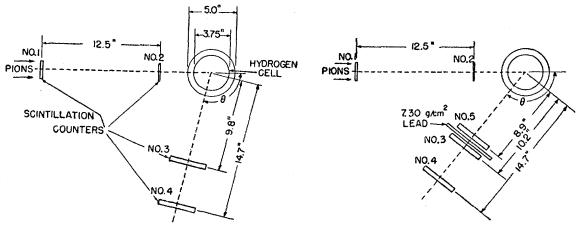

FIG. 1. Details of the scattering geometry. (a) Detection of scattered pions. Counters No. 1, 2, 3, and 4 are in coincidence. (b) Detection of gamma rays. Counters No. 1, 2, 3, and 4 are in coincidence, with counter No. 5 in anticoincidence.

were detected by two 4-inch wide by 6-inch high liquid scintillation counters (No. 3 and No. 4) placed at a variable angle with the incident beam. Gamma rays [coming mainly from the decay of the π^0 produced in reaction (3)] were detected using three 4-inch by 6-inch counters (No. 5, 3, and 4) with 7.30 g/cm^2 of lead placed between counters No. 5 and No. 3. A gamma ray was counted with about fifty-percent efficiency by the quadruple coincidence of counters No. 1, 2, 3, and 4, with counter No. 5 in anticoincidence. Observations were made at six angles. In the observation of scattered pions, absorbers were placed between counters No. 3 and 4 at the forward angles to remove the recoil protons. This amounted to 12.94 g/cm^2 aluminum at 25.7° and 6.19 g/cm^2 at 51.4°.

Pulses from the scintillation counter were fed into a preamplifier, amplified in a two-stage distributed amplifier, fed through some 150 feet of 100-ohm cable into another two-stage distributed amplifier and through a delay box into the coincidence circuits. The output of the coincidence circuits was counted in a Hewlett Packard high-speed decade scaler in cascade with an Atomic Instrument decade scaler.

The efficiency of the scintillation counters detecting the scattered particles was checked by observing: (1) the ratio of quadruple coincidences (counters No. 1, 2, 3, and 4) to double coincidences (counters No. 1 and 2) with the counters in line in the sequence No. 1, 3, 4, and 2, and (2) the ratio of quadruple coincidences (counters No. 1, 2, 3, and 4 in coincidence, with counter No. 5 in anticoincidence) to double coincidences (counters No. 1 and 2) with the counters in line in the sequence No. 1, 2, 5, 3, and 4. Results of measurement (1) were quite close to 100 percent; measurement (2) gave something less than 0.1 percent. The counters and the anticoincidence circuit were therefore taken to be 100-percent efficient.

The incident pion intensity was about 20 000 counts per minute. The scattered intensity was about 3 per minute for most of the measurements. Of this, from 20–70 percent was background which remained when the hydrogen was removed from the cell. A typical measurement would consist of (1) coincidences at 25.7° without hydrogen in the cell, (2) coincidences at 25.7° with hydrogen in the cell, (3) coincidences at 51.4° with hydrogen in the cell, (4) coincidences at 51.4° without hydrogen in the cell, etc., the complete sequence being repeated some five to eight times during one run. The coincidence (scattered pions) and anticoincidence (gamma rays) observations were not mingled; a run consisted of about twenty-four hours running time on the anticoincidence measurement followed by about forty hours running time on the coincidence measurement.

II. EQUIPMENT

a. Scintillation Counters

Counters No. 1 and 2 were made thin so that the energy loss of the pions in them would be small, and so that counter No. 2 would not contribute appreciably to the background by scattering pions into the other counters. Counter No. 1 was a liquid scintillator 2 inches in diameter and $\frac{3}{16}$ inch thick, contained in a Lucite cell with $\frac{1}{32}$-inch windows. The liquid used was phenylcyclohexane with 3 g/liter of terphenyl and 10 mg/liter of diphenylhexatriene dissolved in it.[14] The end of the Lucite cell was shaped to fit the photocathode of an RCA 5819 photomultiplier and good optical contact was maintained with a thin layer of silicone grease. The photomultiplier was housed in a cylindrical mu-metal shield to minimize the influence of the stray magnetic field present. Counter No. 2 was a $\frac{1}{8}$ inch thick, 2-inch diameter plastic scintillator making good optical contact with a Lucite light pipe $\frac{1}{8}$ inch thick. Silicone grease was used for the scintillator-Lucite and Lucite-photomultiplier contact and pressure was maintained to keep the sections in position. The cells of both counters were wrapped in 0.004-inch aluminum foil to increase their optical efficiency. Counters No. 3, 4, and 5 were 4 inches by 6 inches by $\frac{1}{2}$-inch thick over-all Lucite cells with $\frac{1}{16}$-inch windows, containing liquid scintillator; they have been described previously.[5]

b. Electronic Equipment

The pulses from the counters were fed directly from the anode of the photomultiplier into an attached preamplifier[15] which produced pulses of a square shape and about 2.5×10^{-8} second long. After amplification in two distributed amplifiers they went into the coincidence circuits.[15] For the coincidence (scattered pions) measurement, pulses from counters No. 1 and 2 were counted in double coincidence in one circuit F, counters No. 3 and 4 in another circuit B, and counters No. 1 and 3 in a third circuit A. The outputs of these three circuits, which were about 5×10^{-8} second long, were then counted in triple coincidence in a coincidence circuit capable of recording double, triple, or quaduple coincidences. The anticoincidence (gamma rays) measure-

[14] H. Kallman and M. Furst, Phys. Rev. **81**, 853 (1951).
[15] Glicksman, Anderson, and Martin, Proceedings of the National Electronics Conference **9**, 483 (1953).

ment was similar, with the one change being the addition of pulses from counter No. 5 into the anticoincidence input of the double coincidence circuit B. The outputs of circuit F and the triple coincidence circuit each led into a cascade combination of a Hewlett Packard high-speed decade scaler and an Atomic Instrument decade scaler, which then recorded the number D of incident pions and the number Q of interactions, respectively.

The resolving time of the equipment was small enough (2.5×10^{-8} second) to make the number of accidental coincidences a negligible correction. The counting rates were low enough and the dead time of the equipment (about 10^{-7} second) small enough that there was no need to correct the data for counting losses.

c. Hydrogen Target

The hydrogen target differs from one previously described[5] only in the physical dimensions of the scattering cell. The cell has an inside diameter of 3.75 inches and walls of stainless steel 0.005 inch thick. Concentric with it are the radiation shield (0.002-inch thick aluminum) and the external duraluminum vacuum jacket, 5 inches in diameter and 0.015 inch thick. Purified hydrogen gas was used in the transfer of the liquid hydrogen from storage Dewar to target reservoir, and to apply the pressure required to remove the liquid hydrogen from the scattering cell during the experiment.

III. ENERGY OF THE PIONS

The range of the pions in copper was observed by setting counters No. 1, 2, 3, and 4 in line in the beam and measuring the ratio Q/D as a function of the thickness of the copper absorber placed between counters No. 2 and 3. A typical curve obtained is plotted in Fig. 2. To the mean range obtained from this curve is added 1.74-g/cm² aluminum equivalent as the contribution of counter No. 3 and part of No. 4 to the range; 1.02-g/cm² aluminum equivalent is subtracted to represent the contribution of half the hydrogen and the walls of the scattering cell. The result is the mean range of the pions in the center of the hydrogen cell. This is converted to energy using Aron's tables[16] and the value[17] 0.1488 for the ratio of the mass of the pion to the mass of the proton. Two runs were made on the angular distribution of the scattering; in the first of these, the mean energy so obtained was 216 Mev, in the second 218 Mev. The energy spread of the beam was estimated as ±4 Mev in each case. The two runs were averaged and the energy of the average was thus taken as 217 Mev with a spread of ±5 Mev.

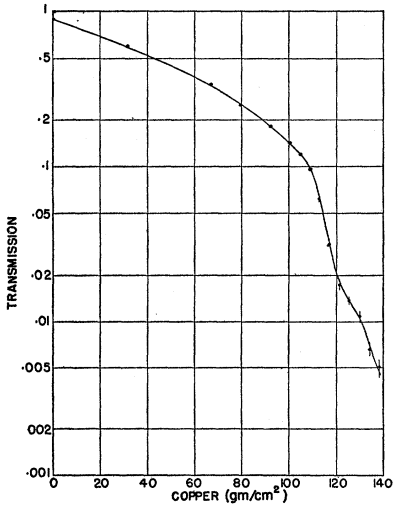

FIG. 2. Range curve in copper taken during Run 2.

TABLE I. Observed values of the fraction (Q/D) of pions interacting to give a gamma ray, in units of 10^{-6}.

Lab angle	With hydrogen	Without hydrogen	Net
	Run 1		
25.7°	530.1±14.5	155.2±9.6	374.9±17.4
51.4°	251.4±10.0	35.4±5.2	216.0±11.3
77.1°	137.4± 7.4	29.7±4.4	107.7± 8.6
102.8°	113.6± 6.7	30.0±4.8	83.6± 8.2
128.6°	140.4± 7.5	45.9±5.5	94.5± 9.3
154.3°	164.4± 8.1	81.1±6.8	83.3±10.6
	Run 2		
25.7°	453.3±18.9	118.7±12.2	334.6±22.5
51.4°	186.5± 9.6	34.4± 6.2	152.1±11.4
77.1°	124.0± 7.9	41.0± 6.4	83.0±10.2
102.8°	106.0± 7.3	25.4± 5.3	80.6± 8.1
128.6°	125.1± 7.9	39.9± 5.5	85.2± 9.3
154.3°	161.5± 9.0	76.5± 7.6	85.0±11.8

Averaged values

Lab angle	Net
25.7°	354.8±20.1
51.4°	184.1±32.0
77.1°	95.4±12.3
102.8°	82.1± 5.8
128.6°	89.8± 6.5
154.3°	84.2± 7.9

From the range curve it is also possible to estimate the purity of the beam. The residual counts after the pions have been absorbed are due to muons (the muon momentum obtained from the range agreeing closely with that of the pions). For the geometry used, multiple scattering corrections to the muon intensity are large. An estimate of these gives 3±1 percent as a value for the muon contamination. A later curve (see Sec. VI) in which the corrections for multiple scattering are small gives a pion content of 97±1 percent, and this value was used throughout.

IV. ANGULAR DISTRIBUTION OF GAMMA RAYS

The experiments of AFMN[5] detected the gamma rays and pions by measuring the coincidences Q/D with and without lead in front of counter No. 3. The measurements without lead included the scattered pions plus some converted gamma rays; the lead measurement included the pions but added about one-half the gamma

[16] W. A. Aron, University of California Radiation Laboratory Report UCRL-1325, 1951 (unpublished).
[17] Smith, Birnbaum, and Barkas, Phys. Rev. **91**, 765 (1953).

TABLE II. Differential cross sections for $\pi^-+p\rightarrow\gamma$.

Laboratory angle θ (deg)	Angle in the barycentric system χ (deg)	Mean gamma-ray energy $\bar{\nu}_l$ (Mev)	Solid angle $\Delta\omega$ (sterad)	Gamma-ray detection efficiency ϵ_γ	Fraction of pions giving gamma ray in units of 10^{-6} Q/D	Differential cross section in laboratory (10^{-27} cm^2/sterad)	Differential cross section in the barycentric system, for γ from π^0 (10^{-27} cm^2/sterad)
25.7	32.9	176	0.110	0.595	354.8±20.1	14.68±0.98	9.31±0.61
51.4	63.9	162	0.110	0.573	184.1±32.0	7.96±1.46	5.98±1.11
77.1	91.9	144	0.109	0.552	95.4±12.3	4.29±0.60	4.03±0.56
102.8	116.7	129	0.109	0.532	82.1± 5.8	3.84±0.31	4.53±0.36
128.6	139.2	118	0.110	0.516	89.8± 6.5	4.31±0.35	6.11±0.50
154.3	160.0	111	0.110	0.516	84.2± 7.9	4.02±0.41	6.40±0.66

rays. Because of the need for using both of the measurements to calculate either of the cross sections for process (2) or (3), the standard deviations of the results are somewhat larger than those for either one of the measurements. It is, however, possible to separate the two processes partially by using the anticoincidence technique described above, which detects only the gamma rays. The results of this give the cross section for production of gamma rays, directly. Not only does this eliminate the increased standard deviation due to the combination of measurements; the much decreased background of the anticoincidence observations increases the accuracy of the measurement itself. The observed values of Q/D for the anticoincidence measurements are given in Table I. The errors quoted are the standard deviations.

The efficiency of the detecting telescope includes a large correction for the scattering and absorption of the electrons in the lead. The scattering correction can be reduced considerably by having the lead as close as possible to the last counter, and this was done here; in the previous experiment[5] the increased background prevented this. The probability of detecting the gamma rays by the electrons or positrons produced in the lead converter was calculated as a function of gamma-ray energy and scattering angle θ, making approximate corrections for the absorption (which decreases the probability) and the large scattering (which increases the probability) of the electrons.[5] These corrections varied from 1.5 percent at the lowest energy to 14 percent at the highest energy. Corrections made in a similar manner in reference 5 gave a calculated efficiency in agreement with a measured value.

The resulting probabilities were multiplied by (a) 0.994 to correct for the gamma rays internally converted[18] and thus not detected, and (b) 0.973 to 0.975 depending on the energy, to correct for the gamma rays converted in the hydrogen, cell walls, and counter No. 5, and therefore not detected. To this was added 0.008 to 0.009 (depending on energy), the probability of conversion in counter No. 3 multiplied by the fraction of gamma rays reaching the counter, to give the probabilities for gamma detection ϵ_γ listed in the fifth column of Table II.

The differential cross section is then given by

$$\frac{d\sigma}{d\omega}=\frac{Q/D}{\epsilon_\gamma(0.993)(0.97)(3.82\times10^{23})\Delta\omega}=\frac{2.69\times10^3}{\epsilon_\gamma\Delta\omega}Q/D,$$

in units of 10^{-27} cm^2/sterad, where the 0.993 is a correction factor due to the attenuation of the beam in passing through the hydrogen, the 0.97 is the fraction of incident particles which are pions, 3.82×10^{23} is the number of hydrogen atoms per square centimeter, and $\Delta\omega$ is the solid angle in steradians subtended by counter No. 4. Observations of the pion flux at the target indicated that the center of the beam did not coincide with the scattering center (see Sec. VI). This gives a small (one to two percent) correction to the solid angle, dependent on the scattering angle θ. Table II contains the pertinent data: θ and χ are the angles of observation in the laboratory system and in the barycentric system, respectively, $\bar{\nu}_l$ is the mean energy of the gamma rays in the laboratory system, and the last column has the contribution of the reaction $\pi^-+p\rightarrow n+\gamma$ (which is estimated from the inverse process[19] as 0.05×10^{-27} cm^2/sterad) subtracted.

The six differential cross sections so obtained have been fitted, using a least squares method[20] by the possible angular distributions

$$d\sigma/d\omega=a+b\cos\chi+c\cos^2\chi, \tag{4}$$

the equivalent

$$d\sigma/d\omega=AY_0+BY_1(\chi)+CY_2(\chi), \tag{5}$$

and

$$d\sigma/d\omega=AY_0+BY_1(\chi)+CY_2(\chi)+DY_3(\chi), \tag{6}$$

where $Y_n(\chi)$ is the nth spherical harmonic. Table III gives the values for the coefficients applicable to the cross sections for gamma rays from the π^0 and for the π^0's. Also included are the values of the weighted least squares sum,

$$M=\sum_{i=1}^{6}\left(\frac{\Delta_i}{e_i}\right)^2, \tag{7}$$

[18] R. H. Dalitz, Proc. Roy. Soc. (London) **A64**, 667 (1951); Lindenfeld, Sachs, and Steinberger, Phys. Rev. **89**, 531 (1953).

[19] J. Steinberger and A. S. Bishop, Phys. Rev. **86**, 171 (1952); White, Jacobson, and Schulz, Phys. Rev. **88**, 836 (1952).

[20] M. E. Rose, Phys. Rev. **91**, 610 (1953).

TABLE III. Angular distribution of charge-exchange scattering.

Process	$d\sigma/d\omega = a + b\cos\chi + c\cos^2\chi$ a	b	c	Weighted least squares sum, M
$\pi^- \to \gamma$	4.32±0.37	1.80±0.38	4.85±0.76	1.35
$\pi^- \to \pi^0$	1.36±0.22	1.23±0.26	4.82±0.76	

Process	$d\sigma/d\omega = AY_0 + BY_1(\chi) + CY_2(\chi) + DY_3(\chi)$ A	B	C	D	Weighted least squares sum, M
$\pi^- \to \gamma$, $D=0$	21.06±0.88	3.67±0.80	5.12±0.80		1.35
$\pi^- \to \gamma$	20.65±1.03	3.55±0.83	5.54±0.96	0.79±1.02	0.78
$\pi^- \to \pi^0$, $D=0$	10.53±0.44	2.52±0.54	5.10±0.80		
$\pi^- \to \pi^0$	10.33±0.51	2.42±0.57	5.51±0.96	1.18±1.52	

$Y_0 = 1/(4\pi)^{\frac{1}{2}}$,
$Y_1 = (3/4\pi)^{\frac{1}{2}}\cos\chi$,
$Y_2 = (5/4\pi)^{\frac{1}{2}}(\frac{3}{2}\cos^2\chi - \frac{1}{2})$,
$Y_3 = (7/4\pi)^{\frac{1}{2}}(5\cos^3\chi - 3\cos\chi)/2$.

which serve as an indication of the goodness of the fit. Here Δ_i is the deviation of the calculated ith cross section from the observed value and e_i is the assigned error to the observed cross section.

If the coefficients for $(d\sigma/d\omega)_\gamma$ are represented by the subscripts γ and those for $(d\sigma/d\omega)_{\pi^0}$ with subscript 0, it can be shown[5] that

$$A_\gamma = 2A_0,$$

$$B_\gamma = \left(\frac{2\gamma}{\eta} - \frac{1}{\eta^2}\ln\frac{\gamma+\eta}{\gamma-\eta}\right)B_0 = 1.464B_0,$$

$$C_\gamma = \left(2 + \frac{6}{\eta^2} - \frac{3\gamma}{\eta^3}\ln\frac{\gamma+\eta}{\gamma-\eta}\right)C_0 = 1.005C_0,$$

$$D_\gamma = \left[\frac{2\gamma}{\eta} + 15\frac{\gamma}{\eta^3} - \frac{3}{2}\left(\frac{5}{\eta^4} + \frac{4}{\eta^2}\right)\ln\frac{\gamma+\eta}{\gamma-\eta}\right]D_0 = 0.666D_0,$$

where η and γ are the momentum and energy of the π^0 in the barycentric system, in units of μc and μc^2, respectively.

Figure 3 is a plot of the two fitted angular distributions, with the experimental points included. Good agreement is obtained with the first three spherical harmonics alone.

V. ANGULAR DISTRIBUTION OF SCATTERED PIONS

The observed values of Q/D for the coincidence measurement are given in Table IV. However, in this case each of these numbers is the sum of: (a) the number of pions emitted into the solid angle multiplied by an efficiency to account for their absorption in the hydrogen, target walls and counter No. 3, and (b) the gamma rays converted in the hydrogen, target walls and counter No. 3. The efficiencies for detecting the pions and gamma rays are included in Table V; the cross sections obtained from the anticoincidence measurement were used in correcting the data for the gamma-ray contribution. Table V is similar to Table II, with the first and second columns giving the angles of observation in the laboratory system and the barycentric system, respectively, the third and fourth columns the efficiencies for detecting the pions (ϵ_π) and the gamma rays (ϵ_γ'), and the last two columns giving the differential cross sections in the laboratory system and in the barycentric system, respectively. The reduced values for ϵ_π at 25.7° and 51.4° are caused by the absorption of the pions in the aluminum absorbers placed in front of counter No. 4 at these angles to keep all recoil protons from reaching the last counter.

The differential cross section in the laboratory is given by the relation

$$\frac{d\sigma}{d\omega} = 2.69\times10^3\frac{(Q/D)_\pi - (\epsilon_\gamma'/\epsilon_\gamma)(Q/D)_\gamma}{\epsilon_\pi\Delta\omega}10^{-27}\ \text{cm}^2/\text{sterad},$$

where $(Q/D)_\pi$ refers to the values in Table IV, $(Q/D)_\gamma$ to those given in Table I. The corrections due to the gamma ray sensitivity are from six to thirteen percent.

As in the case of the gamma-ray measurement, the differential cross sections were analyzed in the form of

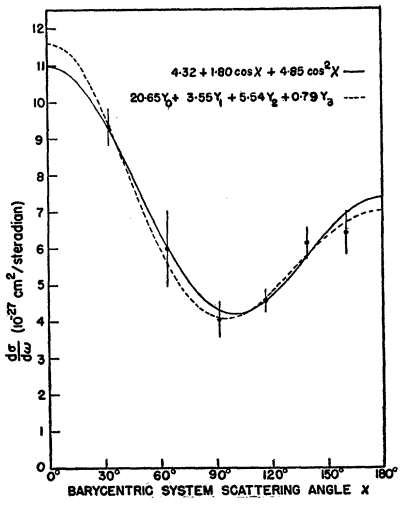

FIG. 3. Differential cross sections of $\pi^- \to \gamma$. The curves are least squares fits to the expressions $a_\gamma + b_\gamma\cos\chi + c_\gamma\cos^2\chi$ and $A_\gamma Y_0 + B_\gamma Y_1(\chi) + C_\gamma Y_2(\chi) + D_\gamma Y_3(\chi)$.

TABLE IV. Observed values of the fraction (Q/D) of pions elastically scattered, in units of 10^{-6}.

Lab angle	With hydrogen	Without hydrogen	Net
	Run 1		
25.7°	840.7±16.0	665.0±16.8	175.7±23.2
51.4°	193.0± 7.5	96.8± 6.8	96.2±10.1
77.1°	125.5± 5.3	83.4± 4.7	42.1± 6.9
102.8°	111.5± 5.3	71.6± 4.9	39.9± 7.2
128.6°	144.2± 5.9	97.5± 5.9	46.7± 8.3
154.3°	248.6± 6.6	194.2± 6.6	54.4± 9.3
	Run 2		
25.7°	587.3±11.2	463.1±11.5	124.2±16.1
51.4°	169.5± 6.3	94.4± 5.4	85.1± 8.3
77.1°	125.7± 5.1	100.1± 4.6	25.6± 6.9
102.8°	105.0± 4.2	78.7± 4.1	26.3± 5.9
128.6°	147.9± 6.1	106.7± 5.5	41.2± 8.2
154.3°	278.4± 8.6	209.2± 7.6	69.2±11.5

Averaged values

Lab angle	Net
25.7°	150.0±25.8
51.4°	90.7± 6.6
77.1°	33.9± 8.3
102.8°	33.1± 6.8
128.6°	43.9± 5.8
154.3°	61.8± 7.4

Eqs. (4) and (6) using a least squares method. The results, including the values of the weighted least squares sum M, are given in Table VI and plotted in Fig. 4.

Rose has shown[20] that M should be about equal to the number of data minus the number of parameters of the fit. For the angular distribution fitted here, M should then be about 3. If it is considerably larger, there are two possible conclusions: either there are systematic errors in the experiment or the fit is being made with too few parameters. Bodansky, Sachs, and Steinberger[4] have made use of the Monte Carlo method to estimate the probability of a given value of M; this analysis gives the result that here M is expected less than 2.3 in 50 percent of the cases. The probability of an M of 4.3 (the s- and p-wave fit) or larger would then be about 20 percent. An analysis of the ordinary scattering is therefore compatible with a small d-wave contribution with coefficient $D=-0.80\pm0.43$; on the other hand the charge exchange scattering was adequately fitted assuming no d-wave contribution.

VI. TOTAL CROSS SECTIONS

The differential cross-section measurements in the laboratory system can be integrated to give the total cross sections for ordinary and charge exchange scattering. Such an integration gives the values in the third line of Table VII. A comparison of these results with a previous angular distribution measurement[8] and a separate transmission measurement[21] indicates some disagreement in the ordinary scattering cross section. A third run was then made, in which the total cross section was measured by a transmission measurement and the differential cross section at 90° for process (2) was also observed at the same time, for pion energies of 209 and 220 Mev.

The electronic equipment and the hydrogen target used were the same as those used in Runs 1 and 2; however, a completely different set of counters was employed. The details of the geometry are given in Fig. 5. Counters No. 1 and 2 were $\frac{1}{8}$ inch thick by 2 inches by 2 inches plastic scintillators, with counter No. 2 three and three-quarters inches from the center of the hydrogen cell. Counters No. 3 and 4 were at 90° to the incident beam direction and counters No. 5 and 6 were in line with the first two counters. Counters No. 3 and 5 were plastic scintillators 7 inches wide, 9 inches high, and $\frac{1}{8}$ inch thick; counters No. 4 and 6 were liquid scintillation counters 8 inches in diameter and $\frac{3}{4}$ inch in overall thickness. Observations were made of the quadruple coincidences (Q) of counters No. 1, 2, 3, and 4, the quadruple coincidences (Q') of counters No. 1, 2, 5, and 6, and the double coincidences (D) of counters No. 1 and 2.

The incident pion energy was measured by taking a range curve in copper as described above. This was done for the incident beam with no absorber and for the case where 5.0 g/cm² of polyethylene was placed in the pion beam between the steering magnet and counter No. 1. The energies of the beams in the two situations were calculated using the mean of the two range measurements and the calculated loss of energy in the polyethylene. The beam without absorber had an energy of 220±6 Mev and the beam with the polyethylene in it an energy of 209±6 Mev, where the ±6 Mev is an

TABLE V. Differential cross sections for $\pi^-+p\rightarrow\pi^-+p$.

Laboratory angle θ (deg)	Angle in the barycentric system χ (deg)	Pion detection efficiency ϵ_π	Gamma-ray detection efficiency ϵ_γ'	Solid angle $\Delta\omega$ (sterad)	Fraction of pions elastically scattered units of 10^{-6} Q/D	Differential cross section in laboratory (10^{-27} cm²/sterad)	Differential cross section in barycentric system (10^{-27} cm²/sterad)
25.7	33.9	0.824	0.026	0.110	150.0±25.8	4.02±0.82	2.42±0.49
51.4	65.7	0.896	0.025	0.110	90.7± 6.6	2.28±0.20	1.67±0.15
77.1	94.1	0.968	0.024	0.109	33.9± 8.3	0.77±0.22	0.73±0.21
102.8	119.0	0.968	0.024	0.109	33.1± 6.8	0.76±0.18	0.93±0.22
128.6	141.0	0.968	0.024	0.110	43.9± 5.8	1.02±0.16	1.57±0.24
154.3	161.0	0.968	0.024	0.110	61.8± 7.4	1.47±0.19	2.62±0.35

[21] Anderson, Fermi, Long, Martin, and Nagle, Phys. Rev. 85, 934 (1952).

estimate of the spread of the beam energy taken from the absorption curve.

A check was made of the beam spread at the hydrogen target using a terphenyl crystal scintillation counter movable in the horizontal direction, with the crystal $\frac{3}{16}$ inch wide by 1 inch high. This distribution was integrated numerically over the cell to give an effective pion length in the hydrogen. This correction amounted to two percent.

From the observations of Q'/D, the cross section was calculated using the expression

$$e^{-N\sigma}=R-r(1-R),$$

where N is the number of hydrogen nuclei per square centimeter, 3.69×10^{23}, σ the total cross section, r the ratio of the number of muons to pions in the beam, 0.03, and R the ratio of Q'/D with hydrogen to Q'/D without hydrogen, 0.98056 ± 0.00073 at 209 Mev and 0.98213 ± 0.00059 at 220 Mev. A number of corrections were made to these values for σ. They have to be increased because of the scattered pions, gamma rays converted in the hydrogen target and counter No. 5, and the protons counted by counter No. 6. These corrections were made using the 210-Mev data[8] and the results reported above; they were about 1.5 percent, less than 0.1 percent, and 2.5 percent for the three kinds of particles, respectively. The values of σ would be decreased by the corrections for the multiple scattering out of the pions in the hydrogen and scattering out of the beam from increased π–μ decay due to the hydrogen. However, these were less than 0.1 percent because of the large angle subtended by counter No. 6 at the hydrogen cell and were neglected. The corrected values for σ are then $57.2\pm2.9\times10^{-27}$ cm^2 at 209 Mev and $52.1\pm2.3\times10^{-27}$ cm^2 at 220 Mev.

TABLE VI. Angular distribution of the scattering $\pi^-+p\rightarrow\pi^-+p$.

$d\sigma/d\omega=a_-+b_-\cos\chi+c_-\cos^2\chi$			
a_-	b_-	c_-	Weighted least squares sum, M
0.85 ± 0.15	0.75 ± 0.22	2.36 ± 0.44	4.33

$d\sigma/d\omega=A_-Y_0+B_-Y_1(\chi)+C_-Y_2(\chi)+D_-Y_3(\chi)$					
	A_-	B_-	C_-	D_-	Weighted least squares sum M
$D=0$	5.80 ± 0.35	1.53 ± 0.44	2.50 ± 0.47		4.33
	5.35 ± 0.43	0.95 ± 0.55	2.01 ± 0.54	-0.80 ± 0.43	0.50

TABLE VII. Total cross sections.

Energy (Mev)	$\sigma(\pi^-\rightarrow\pi^-)$ (10^{-27} cm^2)	$\sigma(\pi^-\rightarrow\gamma)$ (10^{-27} cm^2)	Total $\sigma(\pi^-)$ (10^{-27} cm^2)	Differential cross section at 90° in the laboratory for $\pi^-+p\rightarrow\pi^-+p$ (10^{-27} cm^2/sterad)
210[a]	28.7 ± 3.1	69.1 ± 7.2	$64\ \pm5$	1.47 ± 0.29
217[b]			$60\ \pm6$	
217	18.2 ± 2.3	72.2 ± 6.8	54.5 ± 5	0.76 ± 0.21
209			57.2 ± 2.9	0.86 ± 0.20
220			52.1 ± 2.3	1.03 ± 0.16

[a] See reference 8.
[b] See reference 21.

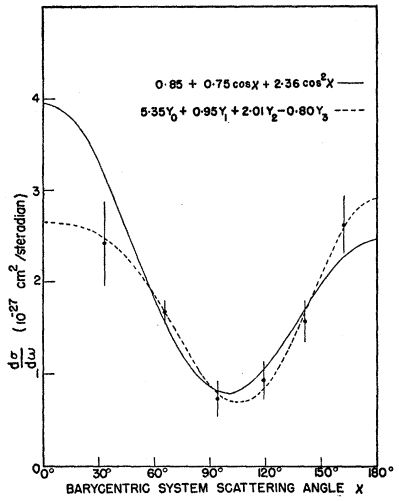

FIG. 4. Differential cross sections of $\pi^-\rightarrow\pi^-$. The curves are least squares fits to the expressions $a_-+b_-\cos\chi+c_-\cos^2\chi$ and $A_-Y_0+B_-Y_1(\chi)+C_-Y_2(\chi)+D_-Y_3(\chi)$.

The observations of Q/D were treated as described previously, and the values of the differential cross-section at 90° in the laboratory system are given in Table VII. The corrections for gamma rays included in Q/D were about eight percent.

The measurements of the total cross section given in Table VII thus seem to agree satisfactorily; there is some indication of a small decrease in the total cross section with energy in this energy interval. The observations of the differential cross section at 90° of the ordinary scattering reported here are all considerably lower than the value at 210 Mev reported previously[8] of $1.47\pm0.29\times10^{-27}$ cm^2/sterad. It would be fair to conclude that the actual value in this interval is of the order of 0.9×10^{-27} cm^2/sterad, and that the figure reported earlier is a high measurement.

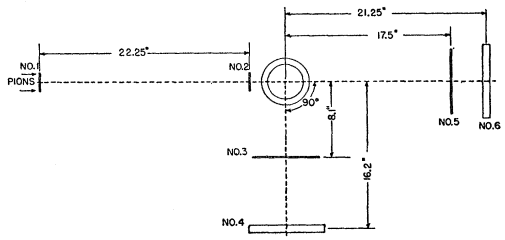

FIG. 5. Details of the geometry used in measuring the total cross section, and the differential cross section at 90° for the process $\pi^-+p\rightarrow\pi^-+p$. Counters No. 1, 2, 3, and 4 are in coincidence; counters No. 1, 2, 5, and 6 are also in coincidence.

TABLE VIII. A few of the possible sets of phase shift solutions to the negative pion scattering data at 217 Mev.

α_3 (deg)	α_1 (deg)	α_{33} (deg)	α_{31} (deg)	α_{13} (deg)	α_{11} (deg)	Total cross sections for π^+ Calculated (10^{-27} cm^2)
20	7	72	12	2	−15	157
20	7	42	−79	−5	−5	160
−69	−3	33	45	4	−12	160

VII. PHASE-SHIFT ANALYSIS

The scattering of pions in hydrogen has been analyzed by AFMN[5] in terms of phase shifts of the states of isotopic spin $\frac{1}{2}$ and $\frac{3}{2}$, and total angular momentum $\frac{1}{2}$ and $\frac{3}{2}$. They find two sets of these six phase shifts which fit the nine data [the coefficients a, b, and c for reactions (1), (2), and (3)] at 120 and 135 Mev fairly well, and these sets are given in reference 5. However, an analysis of the scattering of negative pions in hydrogen at higher energies in terms of these six phase shifts gives a large number of possible solutions because there are only six data to determine the six phase shifts. A graphical method[22] was used to obtain some of these sets as approximate solutions and these are given as examples in Table VIII, along with the predicted total positive pion cross sections. They are approximate in that they were checked against the cross sections to see that the fits were good, but they were not varied to make M go all the way to zero or very near it. With the negative data alone, an analysis using the six phase shifts of s and p waves gives ambiguous results; if d waves are to be included, the situation is still more confusing. The use of positive scattering data would help remove this ambiguity. The present positive data in this energy region consist of the observations of Homa, Goldhaber, and Lederman[11] at 188 Mev, and those of Fowler *et al.*[9] at a mean energy of about 235 Mev but with an energy spread from 210 to 330 Mev. Because of the difficulty of interpolating satisfactorily to data based on such a broad spectrum, an analysis using some interpolation of this data was not made.

Because of these difficulties, it was thought that an analysis in terms of fewer phase shifts might prove interesting. It should be stressed that the author presents this analysis only as an interesting calculation: there is no evidence that the assumption that some of the phase shifts are zero is correct, nor is there a sound theoretical basis for the choices made here.

The phase shifts used in reference 5 were labelled as α_3, α_1, α_{33}, α_{31}, α_{13}, and α_{11} where the first subscript is twice the total isotopic spin, the second is missing for s waves and is twice the total angular momentum for p waves. The results of AFMN[5] indicate that α_{31}, α_{13}, and α_{11} are small in the "first" solution; it was considered worthwhile, seeing how good a fit could be obtained with α_{33}, α_3, and α_1 alone.[23,24] The scattering at 120, 135, 169, 194, and 217 Mev was analyzed in this way; the data used are summarized in Table IX. Here k is the wave number in the barycentric system, and the positive pion values are interpolated from the known data.[9,11,12,25]

As a trial set of phase shifts, α_{33}, α_3, and α_1 were obtained from a graphical analysis[22] using the relations

$$|X+Y|^2=36k^2(a_-+b_-+c_-),$$

$$|X-Y|^2=36k^2(a_--b_-+c_-),$$

$$4\pi\left(a_-+\frac{c_-}{3}+a_0+\frac{c_0}{3}\right)=-\frac{4\pi}{6k^2}\,\mathrm{Re}(X+Y),$$

where the first two equations come from the expressions for the phase shifts, and the last from the "Optical

TABLE IX. Angular distributions used in phase-shift analysis.

	$d\sigma/d\omega=a+b\cos\chi+c\cos^2\chi$					
Energy (Mev)	Process $\pi^-+p\to\pi^-+p$			Process $\pi^-+p\to\pi^0+n$		
	$36\,k^2a_-$	$36\,k^2b_-$	$36\,k^2c_-$	$18\,k^2a_0$	$18\,k^2b_0$	$18\,k^2c_0$
120	1.38±0.31	0.96±0.45	3.28±0.96	0.85±0.56	−2.68±0.71	4.52±2.40
135	2.26±0.45	1.87±0.64	4.48±1.45	1.42±0.73	−3.06±0.81	5.88±3.06
169	3.14±0.93	2.31±1.42	14.93±3.05	4.54±1.77	−1.50±1.52	10.44±5.58
194	5.50±1.18	3.19±1.97	14.10±3.93	4.25±1.97	−0.22±1.82	14.47±6.41
217	4.73±0.85	4.18±1.15	13.14±2.36	3.79±0.57	3.42±0.71	13.42±2.00

Energy (Mev)	Process $\pi^++p\to\pi^++p$		
	$4\,k^2a_+$	$4\,k^2b_+$	$4\,k^2c_+$
120	1.16±0.41	−1.79±0.50	3.67±1.22
135	1.40±0.82	−2.54±1.00	6.45±2.44
169[a]	3.85±1.40	−1.95±1.00	7.3 ±2.3
194[a]	5.20±1.84	−1.3 ±1.0	8.8 ±3.5

[a] It should be noted that the positive data used here do not conform to the requirements of the "Optical Theorem" and analysis for the positive scattering phase shifts (see reference 22); this is due to the asymmetries of the measured angular distributions. The best-fit values, however, do of course satisfy these requirements.

[22] J. Ashkin and S. H. Vosko, Phys. Rev. **91**, 1248 (1953).

[23] The suggestion of an analysis in terms of only these three phase shifts was made to the author by Professor G. Wentzel.

[24] Dr. R. L. Martin of Cornell University has made a similar analysis (assuming however only $\alpha_{13}=\alpha_{11}=0$) using four phase shifts; see R. L. Martin, Phys. Rev. **94**, 765 (1954).

[25] I am grateful to Professor Fermi for making available his analysis and interpolation of the positive pion data.

TABLE X. A set of phase shifts assuming $\alpha_{31}=\alpha_{13}=\alpha_{11}=0$.

Energy (Mev)	Pion momentum in barycentric system η	α_{33} (deg)	α_3 (deg)	α_1 (deg)	Total cross section for π^+ (10^{-27} cm^2) (calculated	Weighted least squares sum M	M (expected)
120	1.24	32	−13	9	100	3.9	6
135	1.33	40	−11	11	121	4.7	6
169	1.51	65	−15	10	174	6.1	6
194	1.63	84	−5	14	184	4.3	6
194		78	−12	−16	179	5.7	6
217[a]	1.76	100	−23	−4	171	8	9

[a] The phase shifts at 217 Mev predict the angular distribution for positive pion scattering: $(d\sigma/d\omega)_{\pi^+}=7.3+5.4\cos\chi+18.8\cos^2\chi$.

Theorem"[22] which states that the total cross section is equal to $4\pi/k$ times the imaginary part of the forward elastic scattering amplitude. X and Y are given by

$$X=e^{2i\alpha_3}+2e^{2i\alpha_1}-3, \quad Y=2e^{2i\alpha_{33}}-2.$$

By using the a's, b's, and c's in the above expressions, a set of three phase shifts can be calculated graphically; these values were then used to try to fit all nine coefficients except at 217 Mev, where they were tested against the twelve measured differential cross sections for negative pion scattering. It was found that the values of M obtained were somewhat insensitive to small variations of the phase shifts, and there is some considerable scatter of the value of α_3, for example. The phase shifts were calculated by numerically minimizing M; this was not exhaustive nor was a search for other possible solutions made. However, at 194 Mev, another similar set giving a poorer fit was found and is included in Table X, which gives the results of the analysis. The signs of the phase shifts were chosen so that α_3 was negative, in agreement with present experimental evidence.[4,26] At 217 Mev, a positive α_3 could correspond to α_{33}, being 80° instead of 100°. The last column gives the value of M expected from the least squares criterion[20] discussed in Sec. V. The total cross sections for positive pion scattering calculated from these best fits are included, as well as the expected values of a_+, b_+, and c_+ for the 217-Mev positive pion scattering. It is seen that all the calculations give fits within the M criterion, indicating that this analysis is a good fit to the data.

The phase shifts obtained in this way are plotted in Fig. 6 against η, the pion momentum in the barycentric system. The phase shift α_{33} behaves as $18°\ \eta^3$ and passes through 90° in the vicinity of 200 Mev; α_3 probably varies as $-8°\ \eta$, and α_1 seems to be a constant 10° with some possibility of a decrease at the highest energy. The behavior of α_{33} in this particular solution would agree with the existence of a resonance in the $\frac{3}{2}$, $\frac{3}{2}$ state as suggested by Brueckner.[27]

In Fig. 7 the positive pion cross sections calculated from the above set of phase shifts are compared to the measured values. The values calculated in the 170–220-Mev region are in agreement with the data presently available. A check of this analysis can be made when positive pion data will be available for comparison of total cross sections and angular distributions in this region.

With a knowledge of the phase shifts it is possible to estimate the influence of the Coulomb scattering on the measured angular distribution: the main contribution at the smallest angle measured is from the interference between Coulomb scattering and the pion-nucleon scattering. A calculation has been made using the three phase shifts alone, as given in Fig. 6, and also using the last of the six phase-shift examples of solutions given in Table VIII. At an angle of 33.9° in the barycentric system the correction is −0.15 or 0.12 $\times10^{-27}$ cm^2/sterad, for the three phase-shift and six phase-shift analyses, respectively; this is to be compared with the observed cross section $2.43\pm0.49\times10^{-27}$ cm^2/sterad. A correction was therefore not made to the data in calculating the coefficients of the angular distribution.

VIII. CONCLUSIONS

The differential cross sections for the processes $\pi^-\rightarrow\pi^-$, and $\pi^-\rightarrow\gamma$ have been measured at 217 Mev and the results fitted using a least squares method to an angular distribution $a+b\cos\chi+c\cos^2\chi$. The fit for the

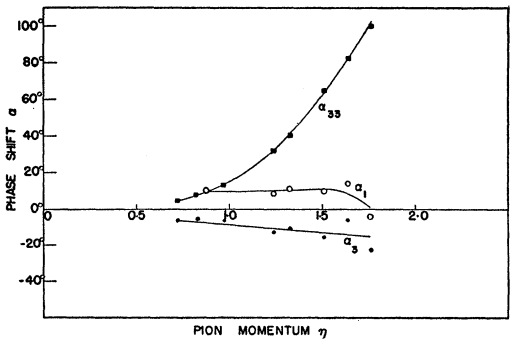

FIG. 6. A possible set of phase shifts obtained by setting $\alpha_{31}=\alpha_{13}=\alpha_{11}=0$, plotted *versus* pion momentum in the barycentric system. The values plotted for $\eta<1.0$ are the solutions of Bodansky, Sachs, and Steinberger, references 4 and 26 (58 and 65 Mev), Orear, Lord, and Weaver [Phys. Rev. **93**, 575 (1954)] (45 Mev), and from AFMN, reference 5 (78 Mev).

[26] Bodansky, Sachs, and Steinberger, Phys. Rev. **93**, 1367 (1954); J. Orear, Phys. Rev. **93**, 918 (1954); Barnes, Angell, Perry, Miller, Ring, and Nelson, Phys. Rev. **92**, 1328 (1953).

[27] K. A. Brueckner, Phys. Rev. **86**, 106 (1952).

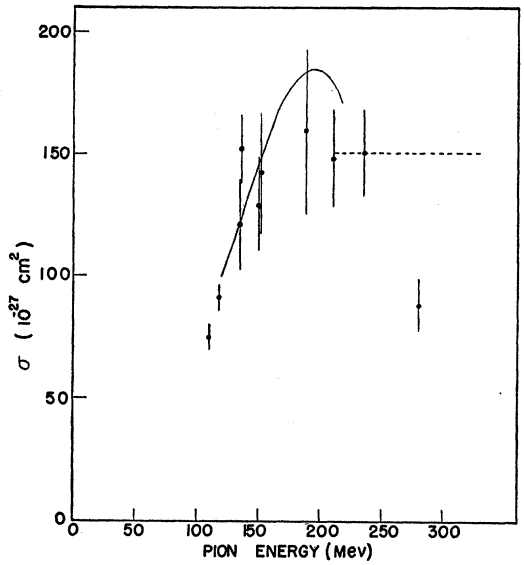

FIG. 7. Total cross sections of positive pions in hydrogen. The curve is that predicted by the three phase-shift sets given in Table X. Experimental values plotted include those of references 5, 9, 11, 12, and 28.

process $\pi^-\rightarrow\gamma$ is excellent, and the experimental results are compatible with assuming no d-wave contribution here. For the process $\pi^-\rightarrow\pi^-$, the fit is only fair, the value of the weighted least squares sum M being 4.3 for six data fitted by three parameters; a value of M as large as this has about 20 percent probability of occurring. Increasing the number of terms of the angular distribution to include p- and d-wave interference gives a good fit; the analysis is compatible with a small d-wave contribution.

A phase shift analysis of the type carried out by AFMN[5] is ambiguous for the negative scattering alone because of the large number of possible solutions. As an interesting exercise, three of the phase shifts were somewhat arbitrarily set equal to zero, and a solution attempted using only α_3, α_1, and α_{33}. Such an analysis gives the curves plotted in Fig. 6. They are presented only as a *possible* set that does represent the data. When accurate data, both of positive and negative pion scattering, become available in this energy region, it should be possible to decide how the phase shifts behave between 135 and 220 Mev.

The integrated total cross sections are $18.2\pm2.3\times10^{-27}$ cm^2 for the ordinary scattering and $72.2\pm6.8\times10^{-27}$ cm^2 for the process $\pi^-\rightarrow\gamma$, giving a value for the total cross section of $54.5\pm5\times10^{-27}$ cm^2. Transmission measurements gave $57.2\pm2.9\times10^{-27}$ cm^2 at 209 Mev and $52.1\pm2.3\times10^{-27}$ cm^2 at 220 Mev, in good agreement with the value obtained from the differential cross sections. These values are also lower than the values $66\pm6\times10^{-27}$ cm^2 at 176 Mev[21] and $74\pm5\times10^{-27}$ cm^2 at 194 Mev,[8] indicating that the cross section has gone through a maximum in this energy region. The observations of Yuan and Lindebaum[28] in the energy range 265–700 Mev give the extent of the drop from the maximum: their results give a total cross section of about 25×10^{-27} cm^2 in the region 340–500 Mev.

Observations of the differential cross section for process (2) disagree with the values obtained earlier at 210 Mev,[8] the measurements at 217 Mev being considerably lower than those at 210 Mev. The cross section was then measured at 90° at 209 and 220 Mev; the results agree with the measurement at 217 Mev and are compatible with the conclusion that the actual value in this energy region is probably about 0.9×10^{-27} cm^2/sterad.

IX. ACKNOWLEDGMENTS

I wish to thank Professor Herbert L. Anderson for his excellent advice and active encouragement throughout this research. I would also like to thank Dr. Ronald L. Martin and Mr. Gaurang B. Yodh for their assistance in assembling the equipment and conducting the experiment, and Mr. Joseph Fainberg for his aid during the experimental runs.

[28] L. C. L. Yuan and S. J. Lindenbaum, Phys. Rev. **93**, 917 (1954).